

Article

Millisecond-Response Nematic Liquid Crystal for Augmented Reality Displays

Jiaxing Tang, Ran Chen *, Zhongwei An *, Xinbing Chen and Pei Chen

Key Laboratory of Applied Surface and Colloid Chemistry (MOE), International Joint Research Center of Shaanxi Province for Photoelectric Materials Science, Shaanxi Key Laboratory for Advanced Energy Devices, Shaanxi Engineering Laboratory for Advanced Energy Technology, School of Materials Science and Engineering, Shaanxi Normal University, Xi'an 710119, China

* Correspondence: tradchenr@snnu.edu.cn (R.C.); gmecazw@163.com (Z.A.)

Abstract: Developing fast-response liquid crystals (LCs) is an essential way to achieve low cost, high resolution, and good visual experience for augmented reality (AR) displays. In this paper, we optimized one new nematic LC mixture SNUP01 to meet the requirements of fast-response phase-only liquid crystal on silicon (LCoS) devices in AR displays. The photoelectric performance of this new LC mixture and three commercial LC mixtures were further comparatively evaluated, and the 2π phase-change response speed of this new LC mixture was extrapolated. The research results indicate that SNUP01 possesses high birefringence, moderate dielectric anisotropy, low viscoelastic coefficient, low activation energy, and high figure of merit values. When using this LC mixture at $25\text{ }^{\circ}\text{C}$ @ $\lambda = 633\text{ nm}$, a 2π phase change can be achieved at 5 V with a total response time of up to millisecond response. Widespread applications of this LC mixture for AR displays are foreseeable.

Keywords: LC mixture; high birefringence; low viscosity; millisecond response; AR displays

1. Introduction

Liquid crystal on silicon (LCoS), as one kind of micro-display technology, combines the unique light modulation properties of liquid crystal (LC) materials with the advantages of high-performance silicon complementary metal-oxide semiconductor (CMOS) technology [1]. Meanwhile, it demonstrates high resolution, low driving voltage, high brightness, and low power consumption, which provides good image quality, suitable pixel size, and high frame rate [2,3]. It is well known that the LCoS technologies are classified into amplitude-modulated and phase-modulated types. In terms of commercialized products, Google Glass and Meta 2 AR glasses have employed amplitude-modulated LCoS devices as micro-displays, while there are some limitations to dealing with 3D information encoding. Due to the excellent light modulation capability of phase-only LCoS [4], it has been one of the attractive hot points in augmented reality (AR) displays [5,6]. For example, both Microsoft and Oculus have used phase-only LCoS devices in their AR prototypes.

In order to improve the resolution of LCoS devices and to overcome motion image blur for AR displays, there is an urgent need to develop millisecond-response LC materials [7,8]. Previous studies have reported that dual-frequency LCs [9], ferroelectric LCs [10], polymer-stabilized LCs [11], and polymer network LCs [12] could achieve millisecond response time. However, these LC materials also have some insurmountable problems. For example, it is difficult to provide continuous-phase grayscale using ferroelectric LCs [13]. Polymer network LCs [14] and polymer-stabilized short-pitch cholesteric LCs [15] both require operating voltages that exceed the maximum voltage (5 V) for the LCoS devices in AR displays. Therefore, nematic LC mixtures have received extensive attention to satisfy these required properties, such as 2π phase change, high resistivity ($>10^{12}$), and low operating voltage ($\leq 5\text{ V}$). In 2017, Chen et al. [16] reported one new LC mixture UCF-N5 with a sub-millisecond response time for AR displays. However, if this LC mixture is



Citation: Tang, J.; Chen, R.; An, Z.; Chen, X.; Chen, P. Millisecond-Response Nematic Liquid Crystal for Augmented Reality Displays. *Photonics* **2023**, *10*, 1062. <https://doi.org/10.3390/photonics10091062>

Received: 29 August 2023
Revised: 17 September 2023
Accepted: 19 September 2023
Published: 20 September 2023



Copyright: © 2023 by the authors. Licensee MDPI, Basel, Switzerland. This article is an open access article distributed under the terms and conditions of the Creative Commons Attribution (CC BY) license (<https://creativecommons.org/licenses/by/4.0/>).

used in a LCoS phase modulator, the response time would likely be four times slower. Huang et al. [17] optimized one new LC mixture, LC-1, to process 2.08 ms response time at a 5.38 V operating voltage for the phase-only LCoS device in AR displays. Subsequently, our group [18] developed a new LC mixture; its high birefringence (Δn) and large dielectric anisotropy ($\Delta\epsilon$) allowed a thin cell gap ($d \approx 1.5 \mu\text{m}$) to be employed in a reflective LCoS device to achieve a 2π phase change at 5 V and a 2.87 ms response time at 40 °C. The growing scientific interest in fast-response LC mixtures for AR displays has inspired us to develop more effective LCs for the phase-only LCoS devices to achieve a millisecond response time.

In terms of the material itself, the response time of LC materials mainly depends on the properties of birefringence, dielectric anisotropy, and viscosity. There are many previous reports about how to achieve high birefringence and low viscosity for a fast response time. For example, Kowordziej et al. [19] employed some LC compounds based on the structure of isothiocyano-tolane to formulate a nematic LC mixture 3071 with high birefringence (>0.3). Previous studies have confirmed that the tolane unit is the most popular chemical structure in LCs to obtain the properties of large birefringence (>0.25) and low viscosity [20–22]. Meanwhile, the lateral fluorine substituent helps to lower the melting point, enhance the nematic range, and improve the dielectric anisotropy [20,23]. The difluoroethylene-terminated groups would contribute to the achievement of low viscosity [24,25].

Based on the above background, in this paper, we selected difluoroethylene-terminated LCs with a high birefringence and low rotational viscosity as the main components of our LC mixture, and further optimized the recipe composition to develop a new nematic LC mixture, SNUP01, through balancing the trade-offs between high birefringence, moderate dielectric anisotropy, and low rotational viscosity. Meanwhile, we further investigated its properties, such as Δn , $\Delta\epsilon$, and viscoelastic coefficient (γ_1/K_{11}). The comprehensive performance of this new LC mixture and three commercial LC mixtures were further evaluated by using the figure of merit (FoM) parameter, and the 2π phase change response speed of this new LC mixture was extrapolated. The research results indicated that this novel LC mixture effectively overcomes the contradictory relationship between low viscosity, moderate dielectric anisotropy, and high birefringence, which is conducive to achieving the millisecond response time at room temperature for phase-only LCoS devices in AR displays. Therefore, widespread applications of this LC mixture for AR displays are foreseeable. This high-birefringence LC mixture with a millisecond response time would also have many potential photonic applications, such as in spatial light modulators, tunable focusing lenses, and electronically controlled phase shifters in the GHz and THz regions [26–28].

2. Materials and Methods

2.1. Characterization and Measurements

The mesocrystalline properties of the LC mixtures were tested using a differential scanning calorimeter (DSC) (Mettler-Toledo, Polaris Pkwy, OH, USA) and a polarizing optical microscope (POM) (LEICA-DM2500P, Wetzlar, German). Heating and cooling rates were controlled using a Linkam THMS600 (Redhill, UK) hot stage. Dielectric anisotropy ($\Delta\epsilon$) values were tested using HP-4274 LCR meter (Keysight, Tokyo, Japan). The birefringence (Δn) values were obtained using phase delay and transient current method [29], and the viscoelastic coefficient (γ_1/K_{11}) values of LC mixtures were tested using the time-dependent transmittance method [30]. A wide nematic phase temperature range for this new LC mixture was confirmed by a DSC instrument and a Haier Ultralow Temperature Freezer DW-86W100 (Haier Biomedical, Qingdao, China).

2.2. Materials

The commercial LC mixture CEJ-1 (noted as P02) was purchased from Xian CaiJing photoelectric technology Co. (Xian, China). Its clearing point is 61.3 °C. The commercial LC mixture E7 (noted as P03) was purchased from Merck KGaA (Beijing, China). Its clearing point is 59.3 °C. The commercial LC mixture HTD028200-200 (noted as P04) was purchased

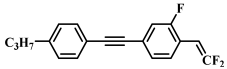
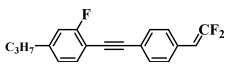
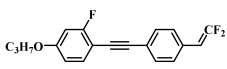
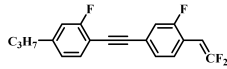
from Jiangsu Hecheng Display Technology Co., Ltd. (Nanjing, China). Its detailed LC performance parameters include a threshold voltage of 1.93 V, saturation voltage of 2.89 V, milky liquid appearance, specific resistance of $\geq 2 \times 10^{11} \Omega\text{-cm}$, and clearing point of 93.8 °C. The LC cells were purchased from the Northern Liquid Crystal Engineering Research and Development Centre (Changchun, China). The difluoroethylene-terminated LCs (3PTGVF, 3GTPVF, 3OGTPVF, and 3GTGVF) were synthesized by us [24], and their GC purities were all above 99.5%.

2.3. Preparation of LC Mixture

In order to meet the 2π phase change for the LCoS devices, high-birefringence LCs and thick LC cells are required. The LC materials with large dielectric anisotropy need to be developed to achieve 5 V driving voltage. To obtain millisecond response time, the LC materials with both high birefringence and low viscoelastic coefficient (γ_1/K_{11}) are required. Therefore, to simultaneously satisfy the above 2π phase change, 5 V driving voltage, and millisecond response time, there is an urgent need to develop nematic LC mixtures with a favorable combination of high Δn , large $\Delta\epsilon$ and low γ_1/K_{11} .

Based on the above analysis, we blended four LC compounds (3PTGVF, 3GTPVF, 3OGTPVF, and 3GTGVF), where the mass ratio of all four compounds was 25%, to formulate a novel LC mixture, SNUP01, with a mass ratio of 1:1:1:1. It is well known that LC mixtures are mainly formulated by mixing a wide temperature modulation component, a high birefringence component, a large dielectric anisotropic component, and a LC diluter. The formulation of SNUP01 is based on the following principles. Compound 3OGTPVF shows a melting point of 55.39 °C, a clearing point of 103.51 °C and a nematic phase temperature range of 48.12 °C, which is suitable to be a wide-temperature-range component. Compound 3GTPVF has a high Δn of 0.285, which is denoted as a high birefringence component. Compound 3GTGVF displays a large $\Delta\epsilon$ of 13.16, which is designated as a high dielectric anisotropy component. Compound 3PTGVF could be used as a LC diluter component to regulate the melting point and viscosity of LC mixtures. As shown in Figure S1, the DSC curve of this LC mixture SNUP01 displays that its clearing point is 59 °C, while its melting point is not detected. Therefore, the storage temperature of this LC mixture is about 5 °C by observing its state in the ultralow-temperature freezer. We put the chemical structure of each component in LC mixture SNUP01, as well as their basic physical parameters, in Table 1.

Table 1. The basic physical parameters of SNUP01.

Compounds	3PTGVF	3GTPVF	3OGTPVF	3GTGVF
Structures				
Percentage	25%	25%	25%	25%
T_m (°C)	43.46	33.67	55.39	19.23
T_c (°C)	no data	61.84	103.51	28.29
Δn	0.284	0.285	0.320	0.243
$\Delta\epsilon$	10.35	7.76	9.75	13.16

3. Results

Considering the fact that the LC mixtures SNUP01, P02, and P03 possess the approximate clearing points, we first tested and evaluated the properties of birefringence, viscoelastic coefficient, dielectric anisotropy, and FoM as a function of temperature and wavelength for these three LC mixtures. Then, we comprehensively evaluated the optoelectronic properties of the LC mixtures SNUP01, P02, P03, and P04 at room temperature, and further screened out the LC mixture SNUP01 with the largest FoM value. Finally, we tested the 2π phase-change speed of the LC mixture SNUP01 and extrapolated its response time for the phase-only LCoS device.

3.1. Birefringence

In this paper, we investigated the variation in Δn with the temperature and wavelength for three kinds of LC mixtures. The voltage-dependent transmittance (V - T) curves were measured using photoelectric characteristic equipment; then, they were converted to obtain the voltage-dependent phase change (V - Φ) curves, and, finally, the Δn values were calculated by using the formula $\Phi = 2\pi d\Delta n/\lambda$ [2]. We filled each LC mixture into a homogeneous cell with the corresponding cell gap $d = 5.1 \mu\text{m}$. They were then fixed onto a Linkam THMS600 hot stage to control the sample temperature. Using a He-Ne laser ($\lambda = 633 \text{ nm}$) as the light source, the Δn values of these LC mixtures were measured during the nematic-phase temperature interval from 10 to 50 °C. Figure 1 shows the temperature-dependent birefringence curves of these LC mixtures, where the dots are the experimental data and the solid lines are the curves fitted by Equation (1) [31]. The test results show that the new LC mixture, SNUP01, has a higher birefringence than those of the commercial LC mixtures P02 and P03 for all the tested temperatures. At 25 °C, the birefringence of LC mixture SNUP01 is 0.275, which is 1.51 times higher than that of the commercial LC mixture P02 and 1.27 times higher than that of the commercial LC mixture P03. Moreover, the birefringence of the LC mixture SNUP01 gradually decreases with increasing temperature, and its Δn is about 0.23 when the test temperature is near the clearing point. Based on the fitting results of the formula, it can be found that the birefringence of the LC mixture SNUP01 at 0 °C (Δn_0) is 0.387. All the fitting parameters are summarized in Table 1.

$$\Delta n = \Delta n_0 S = \Delta n_0 \left(1 - \frac{T_1}{T_c}\right)^\beta \tag{1}$$

where Δn_0 is the extrapolated birefringence at temperature $T_1 = 0 \text{ K}$, S is the molecular order parameter, T_c is the clearing point, and β is the material constant.

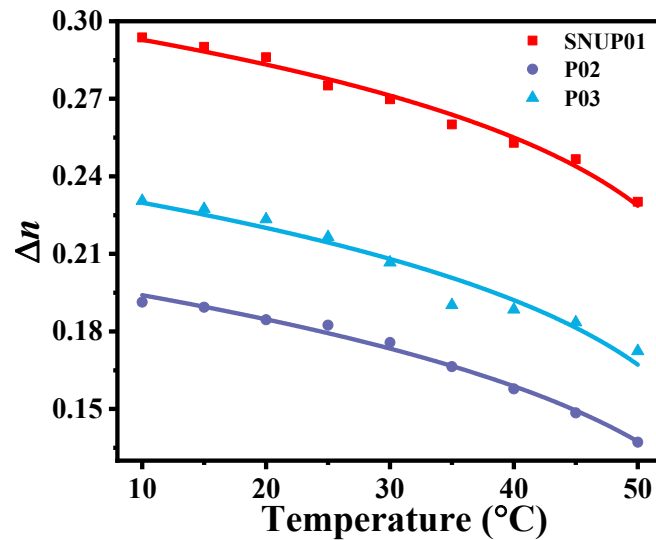


Figure 1. Temperature-dependent birefringence of three LC mixtures at $\lambda = 633 \text{ nm}$.

Meanwhile, to further study the wavelength-dependent birefringence performance, we employed tunable argon ion lasers ($\lambda = 445 \text{ nm}$, 465 nm , and 520 nm) and a He-Ne laser ($\lambda = 633 \text{ nm}$) as light sources to test their Δn values under different conditions. Figure 2a,b shows the wavelength-dependent birefringence curves of these three LC mixtures at 25 °C and 40 °C, respectively, where the dots are the test data and the solid lines are the curves fitted by Equation (2) [32]. The fitting results are summarized in Table 2. At 25 °C and 40 °C, the Δn value of each LC mixture decreased with increasing wavelength at approximately the same change rate. At the same test wavelength, the birefringence of the novel LC mixture SNUP01 was higher than those of the commercial LC mixtures P02 and P03. At 40 °C and a test wavelength of 633 nm, the birefringence of the LC mixture SNUP01 was

0.253, which is 1.60 times higher than that of the commercial LC mixture P02, and 1.35 times higher than that of the commercial LC mixture P03. It can be seen that SNUP01 has a large birefringence at any test wavelength and temperature, which allows it to be applied at different wavelengths of light sources.

$$\Delta n = G \frac{\lambda^2 \lambda^{*2}}{\lambda^2 - \lambda^{*2}} \tag{2}$$

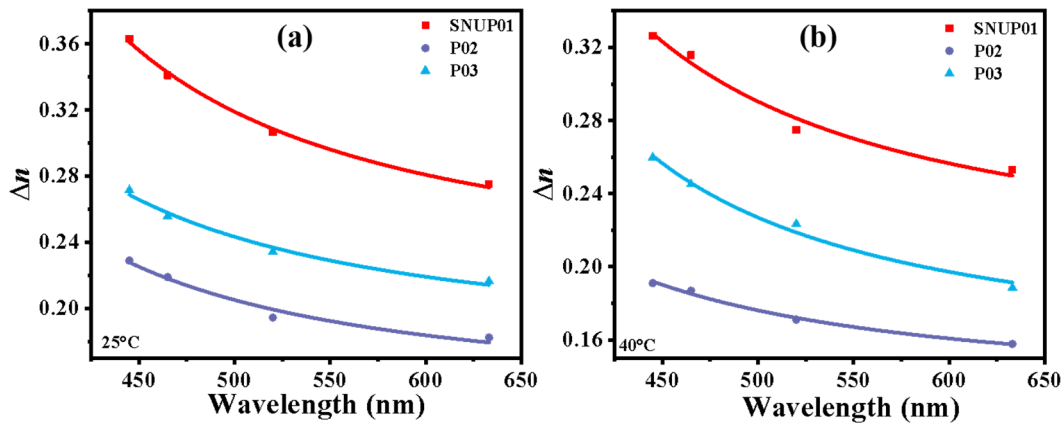


Figure 2. Wavelength-dependent birefringence of three LC mixtures at the test temperature of 25 °C (a) and 40 °C (b).

Table 2. The measured physical properties of three LC mixtures.

LC Mixtures	Δn ($\lambda = 633$ nm)		Δn_0	β	G (μm^{-2})		λ^* (μm)	
	25 °C	40 °C			25 °C	40 °C	25 °C	40 °C
SNUP01	0.275	0.253	0.387	0.146	2.87	2.69	0.277	0.275
P02	0.182	0.158	0.297	0.228	2.15	2.24	0.262	0.244
P03	0.217	0.188	0.331	0.191	2.70	1.84	0.258	0.287

In equation (2), G is the proportionality constant, λ is the test wavelength, and λ^* is the average resonance wavelength.

3.2. Viscoelastic Coefficient

According to the equation $\tau_0 = \frac{\gamma_1 d^2}{K_{11} \pi^2}$ [33], it is known that the response time is directly related to the viscoelastic coefficient (γ_1/K_{11}) of LC materials. The smaller the viscoelastic coefficient is, the faster the response speed is. Therefore, we tested the viscoelastic coefficients of these LC mixtures with the expectation of obtaining one low-viscosity LC mixture. We measured the temperature-dependent viscoelastic coefficient (γ_1/K_{11}) of these LC mixtures by using a He-Ne laser as the light source under the following conditions: test wavelength $\lambda = 633$ nm, test voltage = 10 V, and LC cell gap = 5.1 μm . As shown in Figure 3, where the dots represent the measured data and the solid lines represent the curves fitted by Equation (3) [34], then the corresponding E_a and A parameters were extrapolated to obtain the desired results, which are summarized in Table 3. In Figure 3, the viscoelastic coefficients of these three LC mixtures decreased rapidly at the initial stage as the temperature increased, and leveled off as they approached their clearing points. Compared to the commercial LC mixtures, the new LC mixture SNUP01 has a smaller value of viscoelastic coefficient at any test temperature. For example, the γ_1/K_{11} of the novel LC mixture SNUP01 was 5.93 $\text{ms}/\mu\text{m}^2$ at 25 °C, which was 81% smaller than that of the commercial LC mixture P02 and 63% smaller than that of the commercial LC mixture P03. By extrapolation, the activation energy E_a of these three LC mixtures was obtained, and the activation energy of the novel LC mixture SNUP01 was 238.78 meV, which was

much smaller than those of the commercial LC mixtures P02 and P03. The smaller the value of activation energy is, the faster the low-temperature response speed is [35]. In addition, it can be seen that the viscoelastic coefficient of the new LC mixture SNUP01 decreases gradually with the increase in temperature, and the γ_1/K_{11} value is less than 4 ms/ μm^2 when the temperature tends to the clearing point temperature, and this kind of LC mixture with small viscoelastic coefficient and low activation energy can effectively improve the response time at low temperatures.

$$\frac{\gamma_1}{K_{11}} = A \frac{\exp(E_a k_B T)}{(1 - T/T_c)^\beta} \tag{3}$$

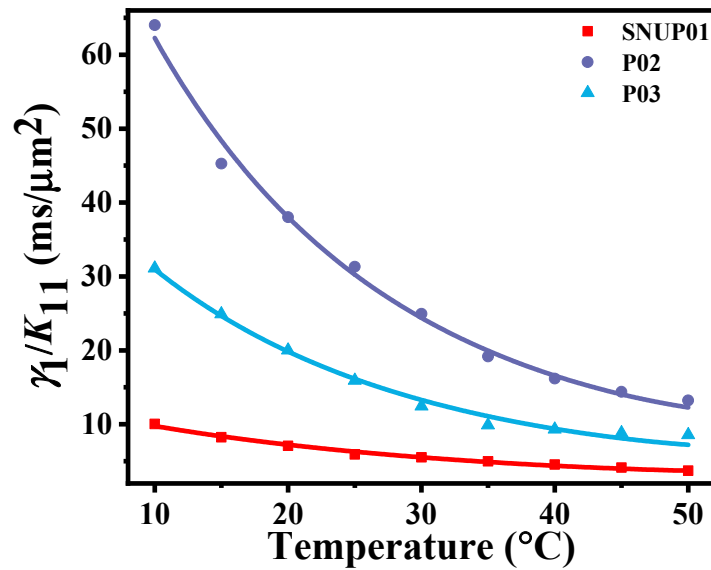


Figure 3. Temperature-dependent viscoelastic coefficient of three LC mixtures at $\lambda = 633$ nm.

Table 3. Parameters related to the viscoelastic coefficient of three LC mixtures.

LC Mixture	γ_1/K_{11} (ms/ μm^2)	A	E_a (meV)
SNUP01	5.93	4.17×10^{-4}	238.78
P02	31.33	5.62×10^{-6}	388.62
P03	15.94	1.29×10^{-5}	350.14

In Equation (3), k_B is the Boltzmann constant, E_a is the activation energy, and A is the proportionality constant, whose values are also summarized in Table 3.

3.3. Dielectric Anisotropy

According to the equation $V_{th} = \pi \sqrt{\frac{K_{11}}{\epsilon_0 \Delta \epsilon}}$, the dielectric anisotropy ($\Delta \epsilon$) of LC materials is inversely correlated with operating voltage [36], and further affects the response time. For the high-resolution LCoS micro-display, its maximum working voltage is limited to 5 V. To reduce the operating voltage, a large $\Delta \epsilon$ LC mixture helps to lower the threshold voltage of the LC device [37]. Herein, we tested the dielectric anisotropy of three LC mixtures, and the results are shown in Figure 4. In Figure 4a, the dielectric anisotropy is linearly dependent on temperature, and the $\Delta \epsilon$ value of each LC mixture decreases with increasing temperature. Among them, the commercial LC mixtures P02 and P03 have larger dielectric anisotropy values, and it can be seen that the dielectric anisotropy value of the new LC mixture SNUP01 is 5.3 at 25 °C.

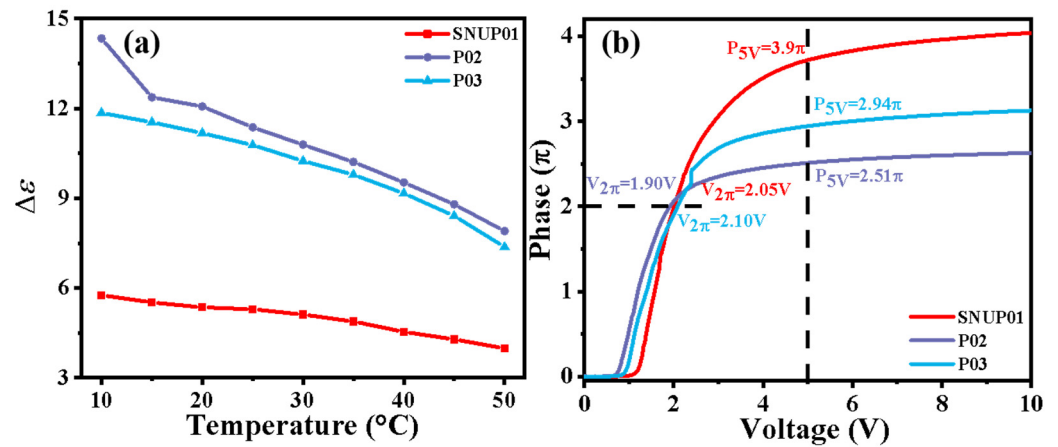


Figure 4. Dielectric anisotropy curve of three LC mixtures with temperature (a); voltage-dependent phase (V - Φ) curve of three LC mixtures at 25 °C (b). The dots represent the measured data.

For better application in the LCoS devices, we chose 5 V as the maximum operating voltage for 2π phase change and calculated the V - Φ curves of three LC mixtures in the LCoS devices. The V - T curves were converted into V - Φ curves at a test temperature of 25 °C and a test wavelength of 633 nm [19], and the results are shown in Figure 4b. The test results indicated that the new LC mixture, SNUP01, can maintain a large phase change (3.9π) at 5 V and a low working voltage (2.05 V) at the 2π phase. In addition, its threshold voltage is 1.3 V. According to the formula $\Phi = 2\pi d\Delta n/\lambda$, when using this LC mixture, the LC cell gap could be reduced to improve the response time while achieving the desired 2π phase modulation.

3.4. Figure of Merit

Figure of merit (FoM) is an important parameter for evaluating LC performance [21,34]. In general, if the FoM value is larger, the response performance of LC material is better [20]. In order to further evaluate the response time of these LC mixtures, we calculated their birefringence and viscoelastic coefficient values according to Equation (4) [34], and obtained their FoM values at different temperatures. As shown in Figure 5, the FoM values of three LC mixtures showed an increasing trend as the temperature increased. However, as the temperature approaches the clearing point, their FoM values drop sharply, which is mainly due to the sharp decrease in their Δn values. The FoM values of LC mixture SNUP01 are much larger than those of the commercial LC mixtures P02 and P03 at any temperatures. Although the Δn and γ_1/K_{11} values of LC mixture SNUP01 both decrease with the increasing temperature, the decreasing rate of Δn is much smaller than that of γ_1/K_{11} , which brings a gradual increase in the FoM values with the increasing temperature. The maximum FoM value of the LC mixture SNUP01 was $14.70 \mu\text{m}^2/\text{s}$ at 45 °C. The maximum FoM values of LC mixtures P02 and P03 were 3.81 and $1.54 \mu\text{m}^2/\text{s}$ at 40 °C, respectively. It is noted that among these LC mixtures, SNUP01 displays the largest FoM value, meaning it is expected to achieve the fastest response time.

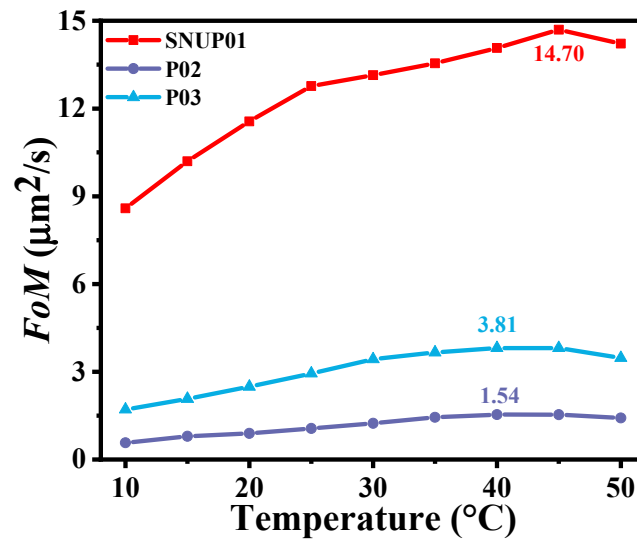


Figure 5. Temperature-dependent FoM values of three LC mixtures. The dots represent the experimental data.

$$FoM = \frac{\Delta n K_{11}}{\gamma_1} \tag{4}$$

In Equation (4), K_{11} is the splay elastic constant, Δn is the birefringence, and γ_1 is the rotational viscosity. All of these parameters are temperature-dependent.

3.5. Comprehensive Evaluations

Based on the above analysis and test results, we further evaluated the comprehensive performance of four LC mixtures, SNUP01, P02, P03, and P04, at room temperature (25 °C) [38]. As shown in Table 4, LC mixtures P02 and P03 have a large dielectric anisotropy (>10) and activation energy (>350 meV), while their small birefringence and large viscoelasticity coefficients lead to small FoM values. Obviously, the viscoelastic coefficient of P03 is nearly half that of P02, making its FoM value large. Compared with P02 and P03, P04 belongs to the high birefringence LC mixture, and possesses a relatively lower dielectric anisotropy and a medium viscoelastic coefficient. Its higher birefringence mainly contributes to a larger FoM value. After the optimization of formulation performance, our new LC mixture SNUP01 presents the highest birefringence, lowest viscoelastic coefficient, and a moderate dielectric anisotropy, which balances the trade-offs among them in the LC mixture formulation. To the best of our knowledge, SNUP01 is a rare LC mixture that could achieve high Δn (~0.28), very low γ_1/K_{11} (5.93 ms/ μm^2), and relatively moderate $\Delta\epsilon$ (5.29) at the same time at room temperature. Therefore, SNUP01 is the most promising LC mixture to achieve millisecond response time for 2π phase change at 5 V operating voltage. In addition, compared to the other three commercial LC mixtures, SNUP01 has the smallest activation energy and largest FoM value.

Table 4. Comprehensive performance of four LC mixtures at 25 °C.

Parameters	SNUP01	P02	P03	P04
Δn	0.275	0.182	0.217	0.262
$\Delta\epsilon$	5.29	11.37	10.77	7.41
γ_1/K_{11} (ms/ μm^2)	5.93	31.33	15.94	16.09
E_a (meV)	238.78	388.62	350.14	268.30
FoM ($\mu\text{m}^2/\text{s}$)	12.77	1.06	2.95	4.27

3.6. Response Time

After a thorough comprehensive evaluation, we screened out the LC mixture SNUP01 as an object for further research to test its response time at room temperature due to the fact that it has the largest FoM value among these four LC mixtures. From Equations (5)–(7) [33], it can be seen that the switching time (rise time and decay time) between two grey levels (V_1 and V_2) for a LC phase modulator is determined by the LC cell gap, viscoelastic coefficient, threshold voltage, and operating voltage. The rise time and decay time curves of SNUP01 at a 2π -phase change voltage ($V_{2\pi}$) are shown in Figure 6a,b, respectively. After careful calculation, the rise response time τ_{on} is 35 ms and the decay response time τ_{off} is 15 ms; therefore, its total response time τ_{total} is 50 ms. To achieve 2π phase change for the reflective cell, the required cell gap is twice as thin as that of the corresponding transmissive cell, which in turn leads to a $4\times$ faster response time. Therefore, the total response time for the reflective cell is 12.5 ms, as shown in Table 5. Since the allowed $V_{2\pi}$ works at 5 V, the required cell gap can be reduced from $5.18\ \mu\text{m}$ to $2.66\ \mu\text{m}$. According to the reference method [39], the extrapolated response time for the rise and decay time is 0.99 ms and 3.94 ms, respectively. After converting the transmissive LC cell to the reflective LC cell, the final total response time for the reflective device at $V_{2\pi}$ is 1.23 ms, which is a $4\times$ faster response time than that of the transmissive device. In the same way, we tested and calculated the extrapolated response times of the other three commercial LC mixtures to the corresponding reflection cells at 2π phase transition and 5 V operating voltage. The response times for P02, P03, and P04 were 10.89 ms, 5.51 ms, and 4.20 ms, respectively. Compared to commercial LC mixtures, the SNUP01 not only has the largest FoM value, but also the fastest response time. Overall, LC mixture SNUP01 can satisfy the phase-only LCoS device to achieve millisecond-response time, 2π -phase change, and 5 V operating voltage for AR displays at room temperature.

$$\tau_{on} = \frac{\tau_0}{(V_2/V_{th})^2 - 1} \tag{5}$$

$$\tau_{off} = \frac{\tau_0}{|(V_1/V_{th})^2 - 1|} \tag{6}$$

$$\tau_0 = \frac{\gamma_1 d^2}{K_{11} \pi^2} \tag{7}$$

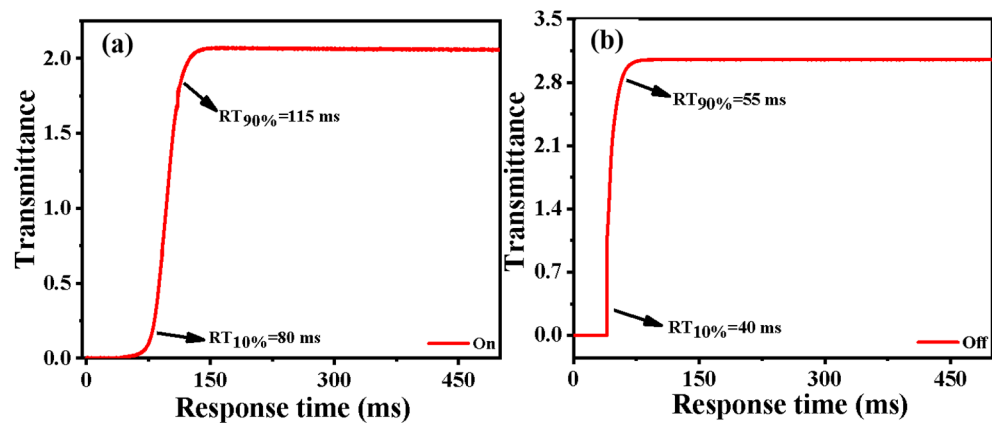


Figure 6. Response time of LC mixture SNUP01 at 25 °C: (a) voltage on, (b) voltage off.

Table 5. Measured response time of transmissive LC cells with $d = 5.18 \mu\text{m}$, and the extrapolated response time to the corresponding reflective cell at 25°C .

LC Mixture	d (μm)	V_{th} (V)	$V_{2\pi}$ (V)	τ_{on} (ms)	τ_{off} (ms)	τ_{total} (ms) Transmissive	τ_{total} (ms) Reflective
SNUP01	5.18	1.30	2.05	35.00	15.00	50.00	12.50
	2.66	1.30	5.00	0.99	3.94	4.93	1.23
P02	5.18	0.69	1.90	36.05	64.00	100.05	25.01
	4.13	0.69	5.00	2.92	40.63	43.55	10.89
P03	5.18	0.88	2.10	31.56	43.06	74.62	18.66
	3.52	0.88	5.00	2.09	19.93	22.02	5.51
P04	5.18	1.13	2.20	56.14	44.22	100.36	25.09
	2.93	1.13	5.00	2.69	14.11	16.80	4.20

4. Conclusions

In summary, we developed a new LC mixture, SNUP01, to achieve a fine balance between high birefringence, moderate dielectric anisotropy, and low viscoelastic coefficient at room temperature. After a thorough comprehensive evaluation, SNUP01 shows a high birefringence (Δn) of 0.275, a moderate dielectric anisotropy value ($\Delta\epsilon$) of 5.29, a low viscoelastic coefficient (γ_1/K_{11}) of $5.93 \text{ ms}/\mu\text{m}^2$, a large figure of merit (FoM) value of $12.77 \mu\text{m}^2/\text{s}$, and a low activation energy (E_a) of 238.78 meV. Therefore, its extrapolated response time to the corresponding reflective cell at 2π -phase change and 5 V operating voltage is 1.23 ms, which satisfies the millisecond response time for the phase-only LCOS devices in AR displays.

Supplementary Materials: The following supporting information can be downloaded at: <https://www.mdpi.com/article/10.3390/photonics10091062/s1>, Figure S1: DSC traces of SNUP01.

Author Contributions: Conceptualization, R.C.; Investigation, Methodology, Software, Data Curation, Visualization, J.T. and R.C.; Writing—Original Draft Preparation, R.C. and J.T.; Writing—Review & Editing, R.C. and Z.A.; Supervision, Z.A., X.C. and P.C.; Funding Acquisition, R.C. and X.C. All authors have read and agreed to the published version of the manuscript.

Funding: The research was funded by the National Natural Science Foundation of China (62105194, 52273186, 51873100); the China Postdoctoral Science Foundation (2022T150394); Sanqin scholars innovation teams in Shaanxi Province, China; and the International Science and Technology Cooperation Project of Shaanxi Province, China (2021KW-20).

Institutional Review Board Statement: Not applicable.

Informed Consent Statement: Not applicable.

Data Availability Statement: The data presented in this study are available in this article.

Acknowledgments: The authors thank those who provided the financial support.

Conflicts of Interest: The authors declare no conflict of interest.

References

- Zhang, Z.; Jeziorska-Chapman, A.M.; Collings, N.; Pivnenko, M.; Moore, J.; Milne, W.I.; Crossland, W.A.; Chu, D. High quality assembly of phase-only liquid crystal on silicon (LCOS) devices. *J. Disp. Technol.* **2011**, *7*, 120–126. [CrossRef]
- Zhang, Z.; You, Z.; Chu, D. Fundamentals of phase-only liquid crystal on silicon (LCOS) devices. *Light Sci. Appl.* **2014**, *3*, e213. [CrossRef]
- Li, P.K. LCOS and AR/VR. *Inf. Disp.* **2018**, *34*, 12–15. [CrossRef]
- Huang, Y.; Liao, E.; Chen, R.; Wu, S.T. Liquid-crystal-on-silicon for augmented reality displays. *Appl. Sci.* **2018**, *8*, 2366. [CrossRef]
- Maimone, A.; Georgiou, A.; Kollin, J.S. Holographic near-eye displays for virtual and augmented reality. *ACM Trans. Graph.* **2017**, *36*, 85. [CrossRef]
- Yin, K.; Hsiang, E.L.; Zou, J.; Li, Y.; Yang, Z.; Yang, Q.; Lai, P.C.; Lin, C.L.; Wu, S.T. Advanced liquid crystal devices for augmented reality and virtual reality displays: Principles and applications. *Light Sci. Appl.* **2022**, *11*, 161. [CrossRef]
- Koulieris, G.A.; Akşit, K.; Stengel, M.; Mantiuk, R.K.; Mania, K.; Richardt, C. Near-eye display and tracking technologies for virtual and augmented reality. *Comput. Graph. Forum* **2019**, *38*, 493–519. [CrossRef]

8. Jin, Y.; Elston, S.J.; Fells, J.A.; Booth, M.; Welch, C.; Mehl, G.; Morris, S. Millisecond optical phase modulation using multipass configurations with liquid-crystal devices. *Phys. Rev. Appl.* **2020**, *14*, 024007. [[CrossRef](#)]
9. Kowrdziej, R.; Wróbel, J.; Kula, P. Ultrafast electrical switching of nanostructured metadvice with dual-frequency liquid crystal. *Sci. Rep.* **2019**, *9*, 20367. [[CrossRef](#)]
10. Gupta, S.; Budaszewski, D.; Singh, D. Ferroelectric liquid crystals: Futuristic mesogens for photonic applications. *Eur. Phys. J. Spec. Top.* **2022**, *231*, 673–694. [[CrossRef](#)]
11. Jeon, B.; Choi, T.; Do, S.; Woo, J.; Yoon, T. Effects of curing temperature on switching between transparent and translucent states in a polymer-stabilized liquid-crystal cell. *IEEE Trans. Electron Devices* **2018**, *65*, 4387–4393. [[CrossRef](#)]
12. Uchida, E.; Ishinabe, T.; Fujikake, H. Local dimming light-guiding plate type backlight system using alignment-controlled polymer-dispersed liquid crystals. *J. Soc. Inf. Disp.* **2017**, *25*, 258–265. [[CrossRef](#)]
13. Srivastava, A.K.; Chigrinov, V.G.; Kwok, H.S. Ferroelectric liquid crystals: Excellent tool for modern displays and photonics. *J. Soc. Inf. Disp.* **2015**, *23*, 253–272. [[CrossRef](#)]
14. Sun, J.; Wu, S.-T. Recent advances in polymer network liquid crystal spatial light modulators. *J. Polym. Sci. Pol. Phys.* **2013**, *52*, 183–192. [[CrossRef](#)]
15. Siemianowski, S.; Bremer, M.; Plummer, E.; Fiebranz, B.; Klasen-Memmer, M.; Canisius, J. Liquid crystal technologies towards realising a field sequential colour (FSC) display. *SID Int. Symp. Dig. Tech. Pap.* **2016**, *47*, 175–178. [[CrossRef](#)]
16. Chen, H.; Gou, F.; Wu, S.T. Submillisecond-response nematic liquid crystals for augmented reality displays. *Opt. Mater. Express* **2017**, *7*, 195–201. [[CrossRef](#)]
17. Huang, Y.; He, Z.; Wu, S.T. Fast-response liquid crystal phase modulators for augmented reality displays. *Opt. Express* **2017**, *25*, 32757–32766. [[CrossRef](#)]
18. Chen, R.; Huang, Y.; Li, J.; Hu, M.; Li, J.; Chen, X.; Chen, P.; Wu, S.T.; An, Z. High-frame-rate liquid crystal phase modulator for augmented reality displays. *Liq. Cryst.* **2019**, *46*, 309–315. [[CrossRef](#)]
19. Kowrdziej, R.; Olifierczuk, M.; Parka, J. Thermally induced tunability of a terahertz metamaterial by using a specially designed nematic liquid crystal mixture. *Opt. Express* **2018**, *26*, 2443–2452. [[CrossRef](#)]
20. Dąbrowski, R.; Kula, P.; Herman, J. High birefringence liquid crystals. *Crystals* **2013**, *3*, 443–482. [[CrossRef](#)]
21. Gauza, S.; Wang, H.; Wen, C.-H.; Wu, S.-T.; Seed, A.J.; Dąbrowski, R. High birefringence isothiocyanato tolane liquid crystals. *Jpn. J. Appl. Phys.* **2003**, *42*, 3463–3466. [[CrossRef](#)]
22. Arakawa, Y.; Kang, S.; Tsuji, H.; Watanabe, J.; Konishi, G. Development of novel bistolane-based liquid crystalline molecules with an alkylsulfanyl group for highly birefringent materials. *RSC Adv.* **2016**, *6*, 16568–16574. [[CrossRef](#)]
23. Kirsch, P. Fluorine in liquid crystal design for display applications. *J. Fluor. Chem.* **2015**, *177*, 29–36. [[CrossRef](#)]
24. Tang, J.; Yao, C.; An, Z.; Chen, R.; Mao, Z.; Chen, X.; Chen, P. Balance the trade-offs between high birefringence, large dielectric anisotropy and low viscosity in nematic liquid crystals through molecular splicing strategy. *Liq. Cryst.* **2023**, 1–9. [[CrossRef](#)]
25. Chen, T.; Liu, M.; Ouyang, H.; Guan, J.; Zhang, Z.; Wang, X. Study on dielectrics and low-temperature viscosity performance of high-frequency difluorovinyl liquid crystals. *Proc. SCIE* **2019**, *10841*, 97–105.
26. Scherger, B.; Reuter, M.; Scheller, M.; Altmann, K.; Vieweg, N.; Dąbrowski, R.; Deibel, J.; Koch, M. Discrete terahertz beam steering with an electrically controlled liquid crystal device. *J. Infrared Millim. Terahertz Waves* **2012**, *33*, 1117–1122. [[CrossRef](#)]
27. Urruchi, V.; Marcos, C.; Torrecilla, J.; Sánchez-Pena, J.M.; Garbat, K. Note: Tunable notch filter based on liquid crystal technology for microwave applications. *Rev. Sci. Instrum.* **2013**, *84*, 026102. [[CrossRef](#)] [[PubMed](#)]
28. Beeckman, J. Liquid-crystal photonic applications. *Opt. Eng.* **2011**, *50*, 081202. [[CrossRef](#)]
29. Wu, S.T.; Efron, U.; Hess, L.D. Birefringence measurements of liquid crystals. *Appl. Opt.* **1984**, *23*, 3911–3915. [[CrossRef](#)]
30. Wu, S.T.; Wu, C.S. Experimental confirmation of the Osipov-Terentjev theory on the viscosity of nematic liquid crystals. *Phys. Rev. A* **1990**, *42*, 2219–2227. [[CrossRef](#)]
31. Haller, I. Thermodynamic and static properties of liquid crystals. *Prog. Solid State Chem.* **1975**, *10*, 103–118. [[CrossRef](#)]
32. Wu, S.T. Birefringence dispersions of liquid crystals. *Phys. Rev. A Gen. Phys.* **1986**, *33*, 1270–1274. [[CrossRef](#)] [[PubMed](#)]
33. Wu, S.T. Design of a liquid crystal based tunable electrooptic filter. *Appl. Opt.* **1989**, *28*, 48. [[CrossRef](#)] [[PubMed](#)]
34. Wu, S.T.; Lackner, A.M.; Efron, U. Optimal operation temperature of liquid crystal modulators. *Appl. Opt.* **1987**, *26*, 3441–3445. [[CrossRef](#)]
35. Chen, H.; Hu, M.; Peng, F.; Li, J.; An, Z.; Wu, S.T. Ultra-low viscosity liquid crystal materials. *Opt. Mater. Express* **2015**, *5*, 655–660. [[CrossRef](#)]
36. Blinov, L.M.; Chigrinov, V.G.; Patel, J.S. Electro-Optic effects in liquid crystal materials. *Phys. Today* **1995**, *48*, 85–87. [[CrossRef](#)]
37. Zou, J.; Yang, Z.; Mao, C.; Wu, S.-T. Fast-Response liquid crystals for 6G optical communications. *Crystals* **2021**, *11*, 797. [[CrossRef](#)]
38. Tang, J.; Mao, Z.; An, Z.; Chen, R.; Chen, X.; Chen, P. Difluorovinyl liquid crystal diluters improve the electro-optical properties of high- Δn liquid crystal mixture for AR displays. *Molecules* **2023**, *28*, 2458. [[CrossRef](#)]
39. Zou, J.; Yang, Q.; Hsiang, E.-L.; Ooishi, H.; Yang, Z.; Yoshidaya, K.; Wu, S.T. Fast-response liquid crystal for spatial light modulator and LiDAR applications. *Crystals* **2021**, *11*, 93. [[CrossRef](#)]

Disclaimer/Publisher’s Note: The statements, opinions and data contained in all publications are solely those of the individual author(s) and contributor(s) and not of MDPI and/or the editor(s). MDPI and/or the editor(s) disclaim responsibility for any injury to people or property resulting from any ideas, methods, instructions or products referred to in the content.